A Microseismic Survey of the Northern Colorado Front Range

John David Godchaux

A departmental honors thesis submitted to the
Department of Geosciences at Trinity University
in partial fulfillment of the requirements for Graduation with departmental honors

May 13, 2000

Thesis Advisor	Department Chair
Glenn C. Kroeger	Diane R. Smith

Interim Assistant Vice President
For
Academic Affairs
Moya A. Ball

Table of Contents

List of Tables and Figures

Abstract

The level of seismicity and the associated seismic hazard in the northern Colorado Front Range is poorly understood. Additionally, the orientation of the modern stress field and the method of seismogenesis for north-central Colorado and southern Wyoming is inadequately constrained. To better understand each of these issues, an array of both broadband and short-period seismometers was deployed encircling the northern Colorado Front Range to measure microearthquake activity.

Thirty-nine local events were recorded by this array during thirty-four days of recording and were subsequently located. Magnitudes ranged from M_{dur} 1.1 to M_{dur} 3.5. Two of these events were determined to be caused by highway road construction on Interstate Highway 80, while the remainder were established to be natural events (earthquakes). Four concentrated linear patterns of events emerged when the event locations were plotted in map view. West of the array, two linear, intersecting patterns of events trending approximately N60˚E and N30˚W plot near, or on top of, mapped faults from Tweto (1979). The trend of these patterns and their angular proximity to the stress field proposed by Zoback and Zoback (1989) for the Denver area suggest that these patterns were created by reactivation along pre-existing faults. Within the array, two other linear, intersecting patterns of events trending approximately N10˚E and N70˚E also suggest that reactivation of pre-existing fractures created these patterns. Also, all four linear patterns of events placed further constraint on the stress field orientation in north-central Colorado.

Acknowledgements

First, I would like to thank Glenn Kroeger for his helpful advise and all of his time spent working through the ever-present computer glitches with me. Much appreciation goes to the Incorporated Research Institutions of Seismology (IRIS), the South-Central Section of the Geological Society of America, and the Department of Geosciences at Trinity University for funding both the field and data processing aspects of this project. I am also grateful to Anne Sheehan for all her help and advise in data collection and subsequent processing. Thanks Ken Dueker, Craig Jones, Lynda Lastowka, Jason Crosswhite, Jason Denotter, and Damon Lytle for their invaluable expertise in field data collection, data formats, and processing. The Kay Ranch, the MacGregor Ranch, the Ryan family, the Mullen family, Joe Smyth, and the NOAA Table Mountain Geophysical Observatory graciously allowed this survey to deploy seismic stations on their property. I would like to express gratitude also to Glenn Kroeger, Walt Coppinger, and the Department of Geosciences for their extensive and constructive revisions along the way. Thanks go to all my family and friends for their support in the hectic times—you forced me to take my mind off of this project, if only for a little while. Finally, I am indebted to the Varsity Squad for the trips to the Coat and the late nights in the lab.

Introduction

The minor amount of historic seismicity and the lack of sufficient microseismic networks for much of the tectonically active western U.S. have lead to an imprecise determination of the seismic hazard (Wong et al., 1996). The possibility of erroneous seismic hazard assessment has great implications for rapidly growing towns and cities in the Rocky Mountain region. One such area is the northern Colorado Front Range. Approximately 2.5 million people reside to the east of this geologic feature.

Historic seismicity in the area has been low, yet two major events have been recorded. First, a M_w 6.6 $\pm$ 0.6 on 7 November 1882 was strongly felt in the northern Front Range region and was located there by Kirkham and Rodgers (1986) and Spence et al. (1996). Second, a cluster of induced earthquakes in the mid-1960s near the Denver metropolitan area was a product of the Rocky Mountain Arsenal high-pressure fluid injection project. Fluids were injected into a 3.7 km deep well triggering several events, the largest of which had a M_S of 4.4 (Herrmann et al., 1981).

Few late Quaternary faults are known in the Front Range. However, this says little about the seismic hazard of the region (Wong et al., 1996). Past microseismic ($M < 4$) monitoring done in the Front Range area (just to the west of Denver) from 1983-1993 by Microgeophysics Corporation showed a moderate amount of microseismicity which tended to occur in swarms (Bott et al., 1996). Two such swarms in western Colorado were studied in detail by Goter et al. (1988; the 1984 Carbondale swarm) and Bott and Wong (1995; the 1986 Crested Butte swarm). Locations of foci (hypocenters) of these swarm related earthquakes appear to trace out planar fault geometries which most likely represent the reactivation of preexisting faults (Bott and Wong, 1995). Although small in magnitude, the number of earthquakes involved in these swarms sums to a significant amount of released seismic energy (Bott et al., 1996).

In the summer of 1999, Godchaux conducted a microseismic survey of the northern Colorado Front Range as an IRIS (Incorporated Research Institutions of Seismology) undergraduate intern. Data were recorded from eleven seismic stations encircling the northern Front Range. The purpose of this study was to further verify the existence of moderate microseismicity in north-central Colorado, and to understand relationship between this seismic energy and the source whether it be natural (earthquake) or otherwise.

Geologic Setting

The Colorado Lineament and the Modern Stress Field. An important Precambrian structural feature of north-central Colorado is the Colorado lineament (Figure 1). As described by Warner (1978), the Colorado lineament is a "Middle Precambrian wrench fault system" trending northeast-southwest and extending from northwest Arizona into east-central Minnesota. Precambrian rocks exposed in north-central Colorado show evidence of faulting and shearing in a well defined belt 160 km wide striking to the northeast (Warner, 1978). Although poorly constrained, the system could have been active as early as 2.0 Ga (Warner, 1978). Following the initial faulting and shearing, this belt has been a zone of weakness within which stresses from ensuing orogenic events have been accommodated (Warner, 1978). Brill and Nuttli (1983) suggested that from 1860 to 1875, eighteen earthquakes with equivalent magnitudes of 4.5 or greater were associated with the Colorado lineament while all other contemporaneous seismicity of this magnitude was associated with other geologic structures. Although historic and modern earthquakes with magnitudes between 3.0 and 4.5 in the Rocky Mountain region appear to be more diffuse, microearthquakes appear to correlate well with the Colorado lineament (Brill and Nuttli, 1983).

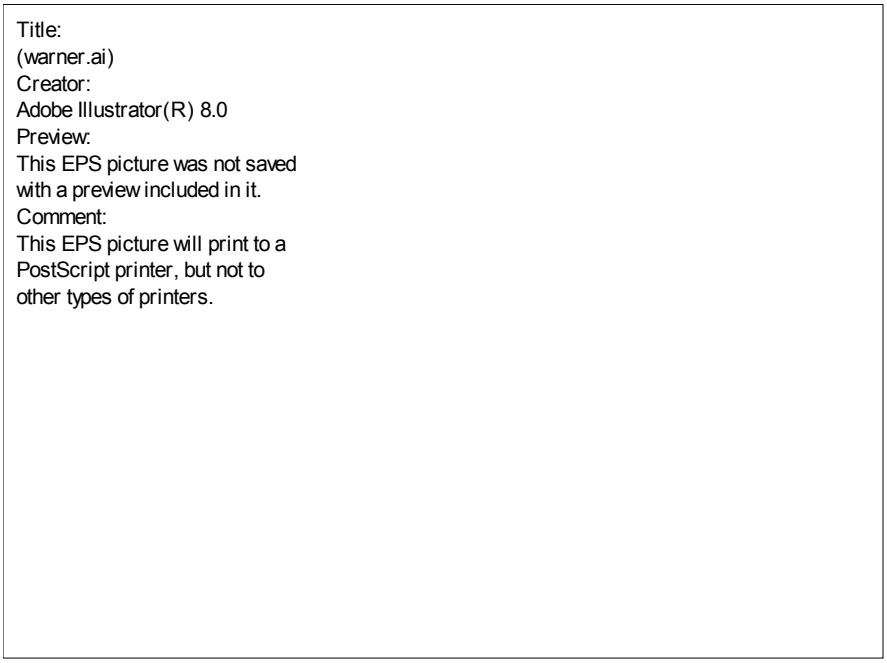

Figure 1. Map view showing the general trend and area of the Colorado lineament (after Warner, 1978).

Zoback and Zoback (1989) described the modern stress field near Denver in north-central Colorado as extensional with the maximum horizontal compressional stress oriented between north and northwest (Figure 2). However, the stress field for most of north-central Colorado and southern Wyoming is poorly constrained. Further constraint of this stress field can be accomplished by recognizing present movements along faults in the area. Faults oriented perpendicular to the modern compressional stress field and hence parallel to the extension direction will show no movement. Any other fault orientation will show movement with maximum displacement on faults oriented approximately forty-five degrees from the maximum compressional stress axis. Compared to past stress fields noted in north-central Colorado and southern Wyoming, the present stress field is relatively weak (Zoback and Zoback, 1989). Given a weak stress field in an area with many pre-existing fractures, it is unlikely that stress will be accommodated by new fractures. It will be accommodated by reactivation of pre-existing faults.

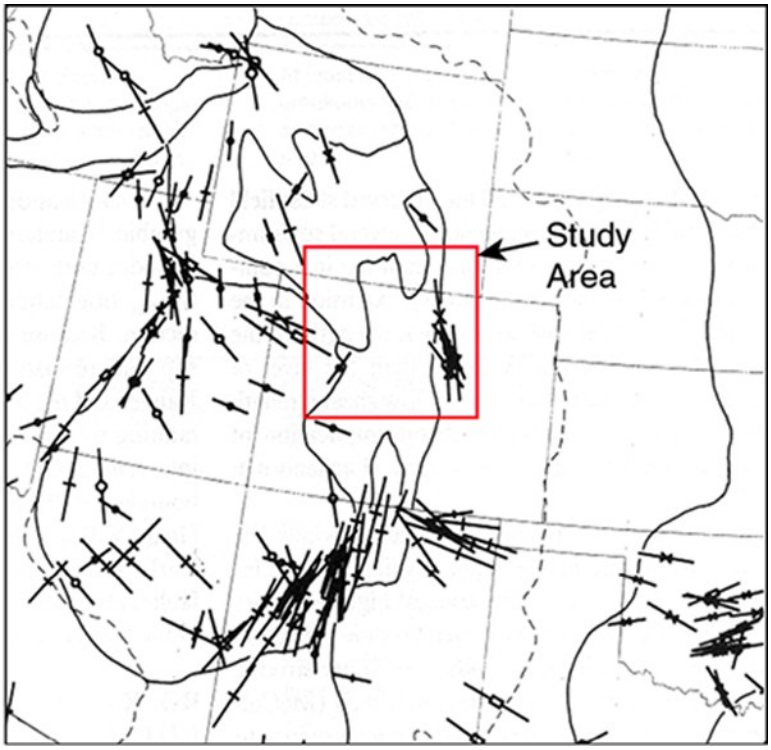

Figure 2. Map of the stress field of Colorado and surrounding states as proposed by Zoback and Zoback (1989). The outline of the study area is in red. The maximum horizontal compressive stress axis is given in the Denver area just east of the Front Range. North-central Colorado, however, has no data on the stress field, but is believed to be extensional in an east-west trending direction. One purpose of this project was to further validate this suggestion.

Historic Seismicity in the Northern Front Range Region. The largest historic event reported in Colorado occurred on 7 November 1882 (Figure 3). The location and magnitude of this event is controversial, but Spence et al. (1996) and Kirkham and Rodgers (1986) located this event somewhere in the northern Front Range. McGuire et al. (1982) tentatively located this event in northwest Colorado, but only utilized local newspaper accounts of felt reports to extrapolate intensity information. Conversely, Kirkham and Rodgers (1986) located this event based on a larger set of intensity data, and also utilized intensity data from a large aftershock on 8 November 1882. Because this aftershock probably occurred at the edge of the mainshock's rupture length, it is likely that both events were less than 20 km apart (Spence et al., 1996). Utilizing the aftershock intensity data, Kirkham and Rodgers (1986) located the aftershock in the northern Front Range, providing good evidence that the mainshock was located there as well. Spence et al. (1996) offered further evidence for this location. Modified Mercalli intensities from the 18 October 1984 Laramie Mountains, Wyoming mainshock (M_b 5.3) and its subsequent aftershocks were compared with intensities from the 1882 events. The spatial coincidence of the intensity patterns for these events is additional evidence for the 1882 mainshock being located in the northern Front Range. Kirkham and Rodgers (1986) and Spence et al. (1996) located the 1882 mainshock to ± 0.5˚ at 40.5˚ N and 105.5˚ W with Spence et al. giving this event an M_w of 6.6 ± 0.6.

In the mid-1960s, a cluster of induced earthquakes related to the high-pressure injection of fluids into a 3.7 km deep well at the Rocky Mountain Arsenal (located slightly northeast of Denver, Colorado) were recorded (Healy et al., 1968). Fluids were injected from March 1962 to September 1963 at a rate of approximately 4.5 million gallons per month (Evans, 1966). Gravity injection resumed 17 September 1964 and continued until the end of March 1965 (1.9 million gallons per month) at which time pressure injection resumed until the end of September 1965 (5.0 million gallons per month; Evans, 1966). The number of earthquakes per month closely followed the volume of fluid injected (Evans, 1966). The more fluid injected, the higher the seismicity. However, these injected fluids affected seismicity approximately 10 days after their injection (Healy et al., 1968).

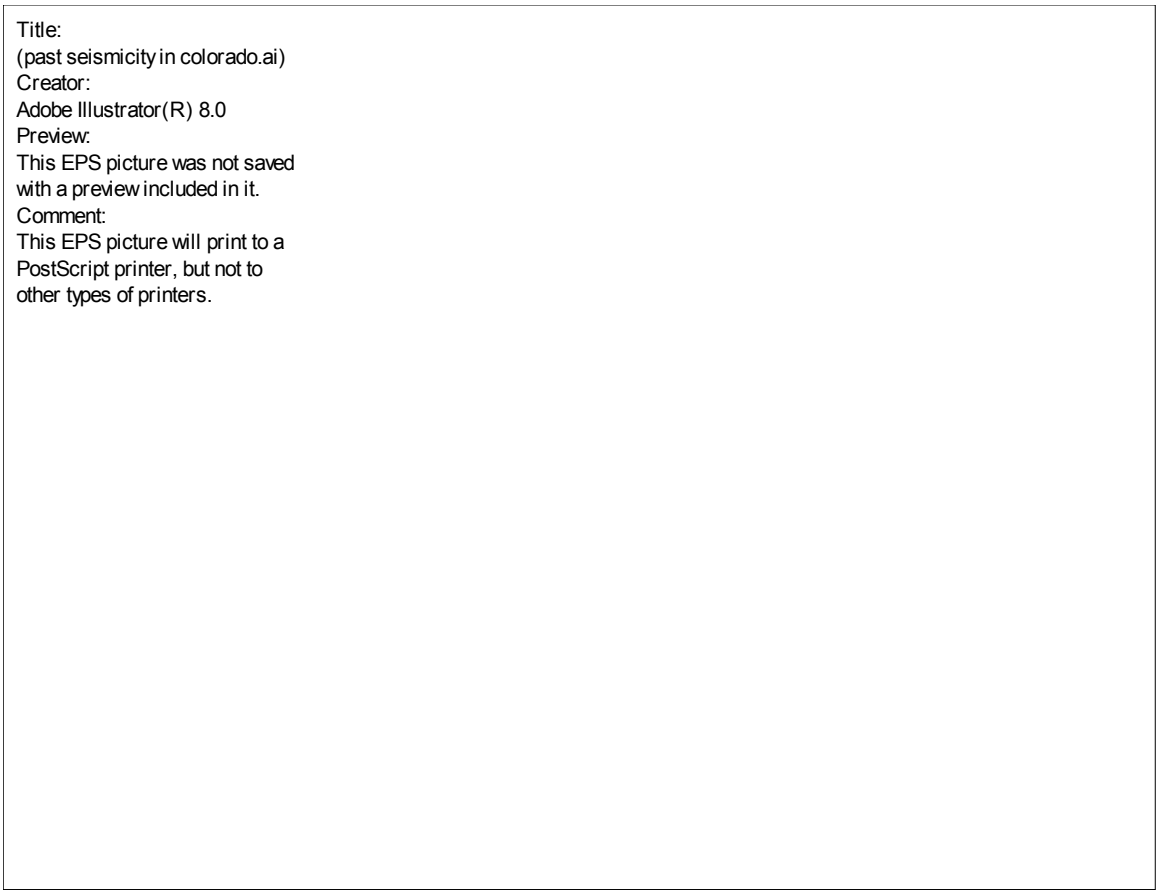

Figure 3. Map of the historic seismicity in Colorado from 1870 to 1992. Dates of significant earthquakes are included along with observed swarming events (after Bott and Wong, 1995).

Earthquake activity continued after injection ceased, and on 10 April, 9 August, and 27 November 1967 significantly large events (M_S of 4.2 ± 0.2, 4.4, and 3.8, respectively) were recorded (Herrmann et al., 1981). Each of these events shook Denver considerably. Aftershocks of the 10 April and 9 August 1967 events defined a line trending approximately N60˚W as did the other induced events (Healy et al., 1968). Depths of 3 to 5 km were assigned to the three mainshocks, and focal mechanisms generally show normal faulting along a fault plane striking northwest (Herrmann et al., 1981). Brill and Nuttli (1983) called attention to the fact that this northwest striking plane is perpendicular to the trend of the Colorado lineament.

Previous Microseismic Studies. From 1983 to 1993, Microgeophysics Corporation monitored the microseismic activity of the central Front Range just west of Denver (Bott et al., 1996). This project discovered a moderate amount of microseismicity and also revealed that

earthquake swarming is the dominant form of seismic activity in the area (Bott et al., 1996). Focal depths of located earthquakes were generally less than 12 km with no events located below 18 km (Bott et al., 1996). A possible correlation exists between the hypocentral locations of events associated with these earthquake swarms and the attitude of Tertiary and Quaternary faults (Bott et al., 1996). Two earthquake swarms in western Colorado, the 1984 Carbondale swarm and the 1986 Crested Butte swarm, show this same correlation with active faults (Bott and Wong, 1995; Goter et al., 1988; Wong et al., 1994).

A very localized microseismic study was conducted by Hughes (1997) in the Boulder-Golden region. Twenty-three events ranging from 0.2 to 2.0 in magnitude were extracted from approximately forty-five days of recording (Hughes, 1997). Notably, Hughes (1997) observed an alignment of located events in a northwest-southeast direction which could be related to activity along a fault. The orientation of this fault is nearly parallel to the fault traced out by the mid-1960s Denver earthquakes.

Methodology

Short Period/Broadband Instruments. Earthquakes or explosions release energy that propagates through the earth in the form of elastic waves (Fowler, 1990). Initially, these waves possess a wide spectrum of frequencies. High frequency or short period waves (approximately 2 Hertz or 0.5 seconds) expend their energy more quickly than low frequency or long period waves (approximately 0.033 Hertz or 30 seconds). Thus, at teleseismic distances (great distances from the energy source) higher frequency waves have either have been greatly reduced in amplitude or are no longer present in the wave train. Conversely, lower frequency waves propagate efficiently to teleseismic distances due to their longer periods.

Different types of instruments are designed to record specific frequency ranges because of the discrepancy in waveforms at varying distances from the source. Short period sensors are designed to record high frequency waves, and consequently, those energy sources which are near the recording instrument (local events). Long period sensors are made for exactly the opposite purpose. These sensors were designed to record low frequency waves, and hence, sources at great distances from the sensor (teleseismic events). Instruments have recently been designed that are capable of recording all frequency ranges. These are called broadband instruments. Though quite expensive, these instruments provide excellent coverage of a wide range of

frequencies pertinent to recording energy from any distance. Although the task of these instruments generally is to record teleseismic earthquakes, the seismograms from these instruments can be utilized in a microseismic survey (such as this survey) since these broadband instruments are capable of recording the high frequencies from local earthquakes.

PASSCAL Stations. A PASSCAL (Program for the Array Seismic Studies of Continental Lithosphere; an IRIS instrumentation program) seismic recording station consists of three main parts: the seismometer, the Digital Acquisition System (DAS), and the Global Positioning System (GPS) clock (Figure 4). The seismometer is essentially a damped spring-mass system in which a magnet is attached to the mass. Surrounding the mass is a coil of wire. As vibrational energy reaches the sensor, the mass and magnet are disturbed. As they move parallel to the coil of wire, the magnet generates an electric current in the coil which is sent as an analog signal (voltage) to the DAS.

The DAS samples the analog stream of voltage from the sensor and digitizes each sample simultaneously. The digital samples are then sent to the DAS' RAM and stored until the RAM is nearly full. The RAM is then dumped to the SCSI disk where the digital samples are archived. This SCSI (Small Computer System Interface) disk was either external (not inside the DAS; utilized by broadband stations) or internal (housed inside the DAS; utilized by short period stations). External SCSI disks hold between one and two gigabytes of archived data while the internal disks hold about 550 megabytes.

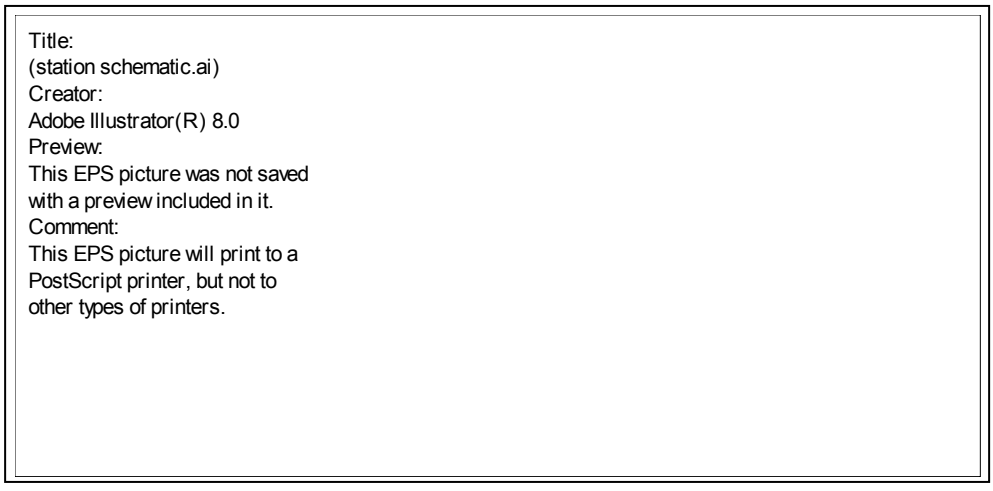

Figure 4. A schematic representation of the functions of the seismometer, DAS, GPS clock, and SCSI disk.

The DAS must assign a time to the digital sample stream that it creates. To make this time as accurate as possible, PASSCAL stations use GPS receivers as clocks. GPS receivers provide a low-cost, low-power method of getting uniform atomic clock accuracy time at all locations in the array. The GPS receiver's function then is to send the accurate time to the DAS once an hour along with position information.

All instruments used in this survey were three component seismometers. Because ground motion is a three-dimensional vector, a complete measure of ground motion requires that all three components of this three-dimensional vector be recorded. Three component seismometers use three separate spring-mass systems oriented orthogonally to record all three components of ground motion. For ease of processing, these spring-mass systems are oriented such that one component records vertical motion, one north-south motion, and one east-west motion.

The DAS can record data in two ways—triggered and continuous. Triggered data are recorded only when the DAS triggering requirement is met. This requirement can be set by the user but is generally set to trigger recording at the first motion (first arrival of energy at the instrument) of an event. The sample rate when recording triggered data is high, but recording only continues for a specified time after the DAS is triggered. Conversely, data acquired continuously are usually recorded at a lower sample rate to keep the external SCSI disk from filling up rapidly. Also, data recorded continuously can be compressed by the Stiem 1 compression algorithm, which can compress data between 2.7 and 3.5 times. All data used in this experiment were recorded continuously.

Survey Instrument Array. In June of 1999, two portable seismograph arrays were installed encircling the northern Colorado Front Range (Figure 5 and Table 1). A combination of seismometers from both arrays were utilized in this study. The first of the two arrays was deployed by the Continental Dynamics—Rocky Mountain project (CDROM). They installed twenty-six PASSCAL broadband seismometers from 5 June through 12 June. These instruments were deployed in a roughly linear array from approximately 30 km south of Steamboat Springs, Colorado to 35 km north of Rawlins, Wyoming. The purpose of the CDROM project is to image the lower crust and upper mantle below this region. Data from five of the CDROM instruments were utilized in this microseismic survey.

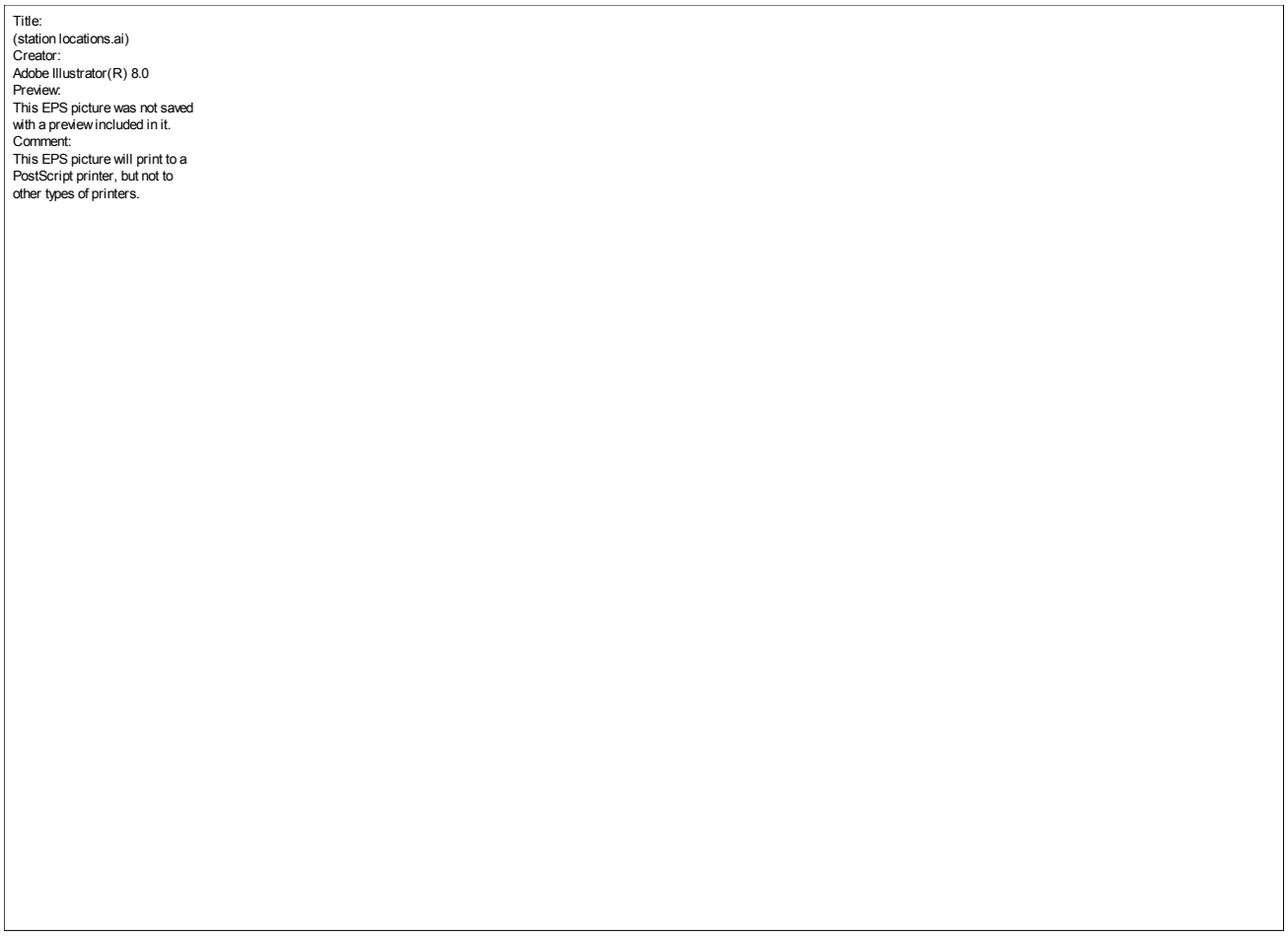

Figure 5. Positions of CDROM broadband stations and L-22 short period stations in north-central Colorado and southern Wyoming used in this study.

The remainder of the array consisted of six short-period seismometers supplied by PASSCAL specifically deployed to record microseismic events in the northern Front Range. These stations were deployed by Godchaux to the north, east, and south of the northern Front Range near the following towns: Silverthore, Boulder, Estes Park, Poudre Park, and Virginia Dale, Colorado; and Laramie, Wyoming (Figure 5 and Table 1). the deployment took place from 14 June through 17 June, with the exception of the site near Silverthore, which was deployed on 29 June. All data acquired by this array were utilized in this survey.

The short-period instruments were utilized because the CDROM array was linear and would not have provided adequate spatial coverage for microseismic location. The deployment of the short-period instruments to the north, east, and south of the northern Front Range created a roughly circular composite array which provided much greater control in data processing.

Because of their proximity to one another (approximately 6 km apart), CDROM data are nearly identical from one station to the next closest station. Because of this, data from only five CDROM stations spread out over the array were used.

Station IDs and towns L=L-22; C=CDROM	Latitude (Degrees north)	Longitude (Degrees west)
L088; Laramie, WY	41.2498	105.6885
L082;Virginia Dale, CO	40.9629	105.3729
L098; Poudre Park, CO	40.6847	105.3030
L085; Silverthorne, CO	39.6648	106.0690
L041; Estes Park, CO	40.3962	105.5209
L048; Boulder, CO	40.1310	105.2326
C861	41.6233	107.2785
C344	40.9249	106.9902
C261	40.2884	106.8243
C057	40.1285	106.6985

Table 1. Station ID, latitude, and longitude of CDROM (broadband) and L-22 (short period) seismic stations used in this study. Towns nearest to the short period station are given.

CDROM Deployment. Two different models of broadband seismometers were used in this project: the Streckeisen STS-2, and the Guralp CMG-3T. Both of these instruments have similar specifications. They share a flat response from 0.0088 Hz to 50Hz and show great sensitivity (1500 volts / meter / second).

At each broadband site, a vault was dug and constructed to house the instrument. These square vaults measured about three-fourths of a meter on a side and one meter deep (Figure 6). Each side of the square hole was lined with one-half inch plywood and about one-half meter of polyurethane foam was stapled to the lid of the vault for insulation. Approximately one-half meter of dirt was used to cover the vault lid for added insulation. Poor insulation of vaults had created significant noise in past data acquired due to expansion and tilting of the ground surface

beneath the instrument. At the bottom of the vault, a layer of concrete was poured on top of hard soil or flat bedrock and horizontally leveled. A ceramic tile was pressed into the wet concrete and leveled. Both the concrete and the tile were positioned so as not to be coupled with the sides of the vault. After the concrete solidified, an orientation marker (either a north or east arrow) was drawn directly on the tile. The instrument was then placed on the tile and oriented correctly.

Figure 6. Lynda Lastowka (left) orients a Streckeisen STS-2 in a vault. At the bottom of the vault is the white ceramic tile with an east arrow drawn for orienting purposes. Instrument specialists from the PASSCAL Instrument Center in Socorro, New Mexico help dig post holes for solar panel stands near Rawlins, Wyoming.

Several feet from the vault, a one-half meter by one meter rectangular hole was dug approximately one-half meter deep. A battery container and an external equipment container were placed in the hole. The battery container housed two marine deep-cycle batteries. The external equipment container housed a REF TEK 72A-08 DAS, a REF TEK external SCSI disk,

a REF TEK GPS clock, and a power board supplied by the PASSCAL instrument center. This SCSI disk holds approximately thirty-five to fifty days of continuous data with the sample rate set to 25 samples per second.

Three Solarex solar panels were incorporated into the system to recharge the batteries. These panels were mounted on solar panel stands that were constructed during the deployment. These stands elevated the panels and allowed them to be oriented correctly to maximize sun exposure. Cabling from the instrument and the solar panels to the external equipment container was wrapped in garden hose and buried to prevent animals from chewing the cabling. Using a Hewlett Packard Palmtop connected to the DAS through the COMM port, each channel coming from the instrument to the DAS was tested by tapping the ground several feet from the vault. The proper parameters (i.e. recording continuously, the appropriate sample rate, etc.) were programmed for each DAS, and the station then began acquiring data. The station acquired compressed data for approximately a month before a crew returned to swap a new, empty external SCSI disk for the full SCSI disk.

Short Period Seismometer Deployment. The Mark Products L-22 seismometer used in this survey is a short period instrument designed to record the frequencies of local, natural events (local earthquakes). Although not as sensitive as the broadband instruments, the L-22 is an excellent sensor for gathering local earthquake data. It boasts a narrow response curve with a peak response at about 2 Hertz or 0.5 seconds. The sensitivity of these instruments is 88 volts/meter/second.

The DAS connected to the L-22 is a REF TEK 72A-07 model and differs from the A-08 model in that it contains an internal SCSI disk. This disk holds approximately twenty to thirty days of continuous data at 25 samples per second. Moreover, the short period stations were powered by a 110 Volt AC electrical outlet instead of batteries. Since the DAS needed DC power to operate, an AC/DC converter was employed between the AC outlet and the power board input. Being required to use an AC outlet greatly limited where the stations could be placed and probably introduced considerable noise into the data. With the exception of the station deployed near Boulder (deployed at the NOAA Table Mountain Geophysical Observatory), all stations were placed on private property near buildings with AC outlets.

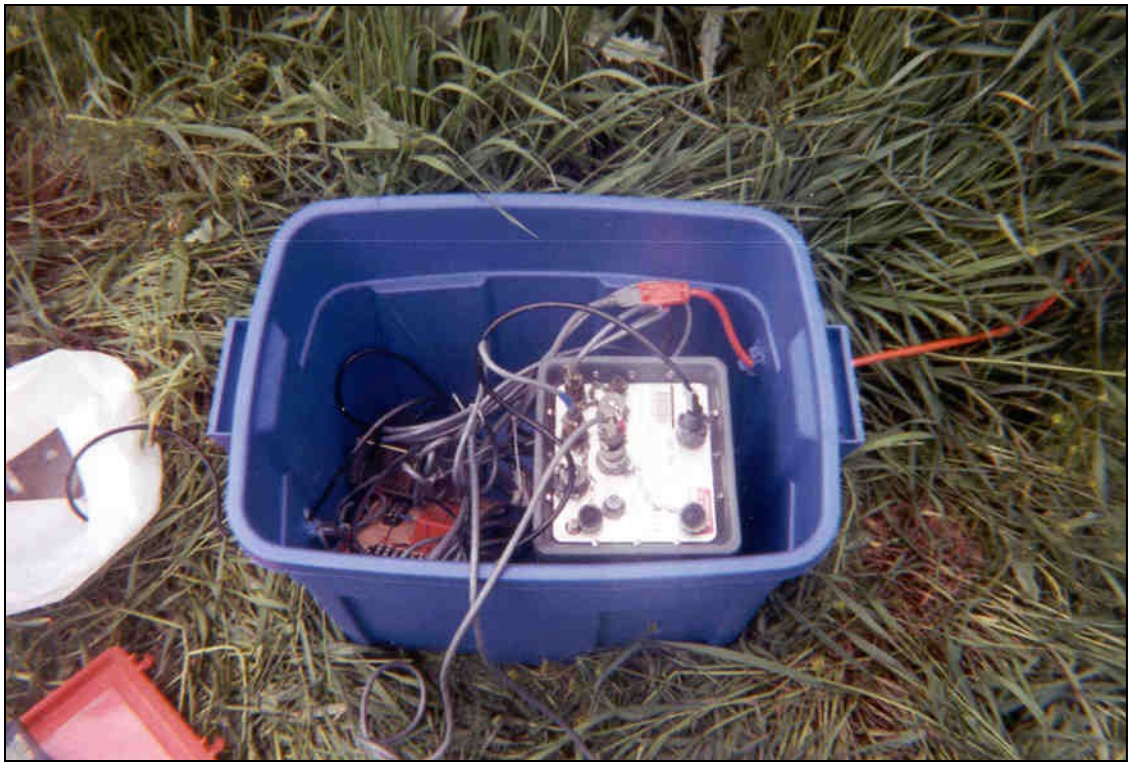

Figure 7. At a short period site, large Rubbermaid containers housed the DAS, GPS, and AC/DC power converter. The ports on the DAS are shown facing up. Off to the right, an extension cord leaves the container and plugs into a conventional AC wall outlet. To the left, the mark products L-22 seismometer is inside the plastic bag, and the Hewlett Packard Palmtop computer is just out of the picture in the lower left corner.

The short-period stations were deployed in the following manner (with the exception of the station at the NOAA Table Mountain Geophysical Observatory). To house the instrument, a small cylindrical hole approximately a foot in diameter and ten inches deep was dug and the bottom leveled. The instrument was then put in a plastic bag, placed in the hole, oriented, and leveled. The REF TEK 72A-07 DAS, REF TEK GPS clock, and AC/DC power converter were placed in a large Rubbermaid container (Figure 7). This container was placed one to four meters away from the seismometer. A tap test was preformed as described previously, and the proper parameters were set. During the initial deployment of these stations, the dataform field in the parameters menu was set to 32-bit instead of compressed (COM). This meant that the first data acquired were uncompressed data. The significance of this condition will be addressed later. Acquisition of data was then started, and the site was checked for equipment protection and exposed cable.

In contrast to the other short-period stations, the L-22 station deployed at the NOAA Table Mountain Geophysical Observatory was placed inside the Geophysical Observatory building. The seismometer was placed on a "pier" which is a rectangular block of concrete with one-by-one meter sides and an approximate height of three meters. This pier has been driven in the ground such that a top surface of the concrete block is level with the floor of the building. Around the pier is approximately six centimeters of foam damping any movement of the building. A USGS geodetic bench mark is in the center of the pier. The seismometer was leveled, and was oriented with the USGS geodetic marker. The GPS unit was placed in a plastic bag outside on cinder blocks. The GPS cable was threaded through a machined hole in the wall with PCV pipe lining the hole. Initialization followed as described for the other short period stations.

Visitation and Troubleshooting. From 5 July until 9 July 1999, the short period stations were visited and the data stored on the internal SCSI disk were downloaded to a portable Linux laptop supplied by PASSCAL. This process was easily accomplished by stopping the DAS acquisition, physically connecting the laptop to the DAS, and programming the laptop to download the data using the *diskdump* command from the PASSCAL database (*pdb*) package. This package of programs was written by PASSCAL to facilitate database management. The dataform parameter was changed to COM or compressed, acquisition was re-initialized, and the station was departed.

Several instrumentation problems were dealt with during data recording. First, due to a faulty DAS unit, the Silverthorne site was not deployed until 29 July. Second, upon returning to the Virginia Dale site both during the first data pick-up and when the site was taken down, the DAS' RAM was found in ASLEEP mode. This means that the DAS had stopped recording, but the source of this problem was never discovered. Recording on this station began 14 June and stopped 19 June, but was re-initialized on 8 July only to stop again on 19 July. Finally, the site near Laramie, Wyoming ceased recording after only several hours due to a bad AC/DC converter. This site was returned to normal functionality when a new AC/DC converter was installed during the first data pick-up. All short period stations were withdrawn from 26 July through 28 July 1999.

Data Formats. After the retrieval of the first set of data, processing began at the University of Colorado-Boulder. Event picking at this point was tenuous since data from only three short period sites were available. Therefore, most of the data processing took place at Trinity

University. However, data were converted from raw REF TEK format to SEGY or miniSEED (mSEED) format while in Colorado. SEGY (Society of Exploration Geophysicists—Format Y) volumes were written from raw REF TEK packets when data were recorded uncompressed. This included the first set of data recorded by the first five short period instruments deployed. MiniSEED format, which is a descendent of the Standard Exchange of Earthquake Data (SEED) format, was written from raw REF TEK packets when data were originally recorded in a compressed format. MSEED format was written for the remaining short period data and for all broadband data. Having been converted into a readable format, these files and their corresponding raw REF TEK packets were copied to DAT tape and transferred from Colorado to Trinity University.

Data Processing. At Trinity University, SEGY and mSEED data were transferred from DAT tape to a PC running RedHat Linux 6.0. The *pdb* database manager was downloaded to the PC also. Within *pdb* are a set of programs written for data conversion and processing. One such processing program is called PASSCAL Quick Look (*pql*), which is a seismic trace viewer. *Pql* allows for viewing and some processing of seismic traces in both SEGY and mSEED format, but only one format can be plotted when running the program. Also, *pql* plots up to 100 time-overlapping one-hour trace segments. Both SEGY and mSEED formats store data by breaking the continuous traces from each channel of the DAS into one-hour segments.

The SEGY and mSEED files created at the University of Colorado-Boulder originated from a SUN Ultra-10 workstation. Consequently, these files were created with big-endian byte ordering. Because the Intel PC running Linux is reads and writes only little-endian byte ordering, the SEGY and mSEED files created by the SUN had to have their byte ordering reversed or swapped to be used on PC Linux. Fortunately, the *pdb* package contains a program called *segysun2pc* which swaps the byte ordering of a SEGY file from big-endian to little-endian. Unfortunately, *segysun2pc* was unreliable on the Linux platform. When converting some SEGY files a memory leak would cause the program to crash and erase the original file.

Byte ordering information of SEED (and mSEED) files is located in the header of each file. Programs using these formats should be able to read this information and convert the file to whichever byte ordering scheme is applicable. For whatever reason, *pql* could not do this on mSEED files.

Since *segysun2pc* was having difficulty swapping the byte order of some SEGY files and *pql* could not plot mSEED files, the PC-based Linux machine was abandoned in favor of a SUN SparcStation 20 running Solaris 2.5.1. All data were subsequently transferred to the SUN workstation.

At this point, it was discovered that one CDROM station (C097) had experienced extensive GPS problems while recording. The GPS was to provide the only reliable time measurements for each station, and without an accurate time clock, significant clock error could not be corrected. Therefore, this station could not be used in data processing and was abandoned.

Filtering of the continuous data for local events was done exclusively in *pql*. In the initial pass through the data, any significant energy that appeared at more than a few stations was considered more carefully later. Files containing no significant energy were erased from the disk. After this first pass, all of the mSEED data were uncompressed and converted to SEGY format using the *pdb* program called *mseed2segy*.

Following the data conversion, the picked events were sorted into categories of general distance from the source to the array. Each event was categorized as a local event (source was within or very nearby the array), a regional event (source was from a moderate distance away), or a teleseismic event (source was from a great distance away). Events were to be categorized on the basis of the time difference between P-wave (primary wave) and S-wave (secondary wave) arrivals. The larger this time difference was, the farther away the source must be from the array. Another criteria for categorizing was the presence and position of surface waves in the CDROM records. Surface waves that were separated in time considerably from the S-wave and were long in time duration indicated a teleseismic event. However, this categorizing was done with caution because the P-wave was sometimes hidden or difficult to see, and the S-wave might have been mistaken for the P-wave in these situations.

For each local event, a P-wave arrival time was extracted for each station on which the event was detected. Also, one S-wave arrival time was taken from each event to constrain the depth of the hypocenter. These arrival times were used in the program *HypoInverse* (Klein, 1978), which is a program created by the United States Geological Survey for hypocenter location. To run *HypoInverse*, three tables of information must be created: an arrival time table, a station table, and a crustal model table. The station table simply assigns each station an ID code and contains each station's geographic location. Also, the station table allows the programmer to weight the

quality of a station recording for all events recorded by a given station. This was done for the station in the town of Poudre Park, Colorado (L098) which was given half the value of all other stations due to excessive noise on the vertical channel. The arrival time table consists of the P-wave arrival times from each station with one clean S-wave arrival time from a selected station that provides a strong depth constraint. Each station in this table is assigned an ID code which then can be correlated to the geographic location information located in the station table. The arrival time table also allows weighting of the trace's quality. Most of the weighting was done by this method. For most events every trace was given full weight. Finally, the crustal model table identified the crustal model used in processing (Table 2).

P-Wave velocity (km/s)	Depth to top of layer (km)
5.70	0.0
6.00	8.3
6.70	27.0
7.90	49.0

Table 2. Crustal velocity model appropriate to western and central Colorado (after Wong, 1991).

To test *HypoInverse*, a designed "event" of known location was programmed into the locating program. Four stations were given locations at the corners of a square and all stations were provided with the same arrival time. *HypoInverse* correctly located the "event" at the center of the square.

An initial set of locations was obtained using a single layer model with a P-wave velocity of 6.0 km/s. Because the locations returned by *HypoInverse* were reasonable, a three layer over halfspace crustal model pertinent to western and central Colorado (Wong, 1991; Table 2) was employed for the final locations. These locations were then plotted in ArcView 3.2 GIS (Geographical Information System; a mapping program which allows querying of geospatial datasets). Pertinent faults from Tweto (1979) were digitized into the GIS using a CALCOMP 9100 digitizing tablet.

Magnitude Calculations. Duration magnitudes (M_{dur}) were calculated for eighteen events located by *HypoInverse* (Appendix 1). Calculating duration magnitudes is a useful way to estimate the magnitude of microearthquakes since records for these earthquakes are seldom

useful (Lee and Stewart, 1981). The duration or coda length of a seismic event is the amount of time elapsed between the first arrival of energy and the point at which the signal (mostly surface waves) decays to two times the background noise (Sheehan, 2000). Calculation can be done according to the following equation:

$$M_{dur} = a_1 + a_2 \log(\text{coda length}) + a_3\Delta + a_4 h \qquad \text{(Equation 1)}$$

where Δ is the epicentral distance of the event to the station in kilometers, h is the focal depth in kilometers, and a_1, a_2, a_3, and a_4 are empirically derived constants (Lee and Stewart, 1981). It has been noted by Lawson (personal communication) that usually the empirical constants a_3 and a_4 are small enough that their respective terms can be ignored for a local microearthquake network. Therefore, duration magnitude can be calculated independent of distance and depth to the hypocenter.

The coda length or duration of a seismic event varies depending upon the station used; levels of background noise from station to station differ. It is important to note here that this survey decided to use both the coda length as defined by Sheehan (2000) and also the complete duration of a seismic event (the elapsed time from the P-wave to the point at which the signal cannot be distinguished from the noise). This was done to provide a check on the original duration magnitude.

Coda lengths were first measured for eleven events on all stations. These eleven events were used for two reasons. First, the events were recorded by this survey and the USGS NEIC (National Earthquake Information Center). This gave reference magnitudes (M_L) calculated by the USGS which were correlated with the coda lengths of each event. Second, events were also chosen on the basis of their overall quality.

The base ten logarithm of coda length for each event was plotted against the USGS calculated magnitude in Microsoft Excel. For each station separately all eleven events were plotted and a linear regression analysis was performed. This created two duration magnitude scales (one for the full decay of seismic energy into the background noise and the other for the decay of energy to twice the background noise) for each station in which to calculate magnitudes for events not analyzed by the USGS. This magnitude scale was of the following form:

$$M_{dur} = a_1 + a_2 \log(\text{coda length}) \qquad \text{(Equation 2)}$$

where a_1 and a_2 are station specific and are calculated in the regression analysis. Because the regression analysis produced good correlation between duration and calculated USGS magnitude on three stations, only these three stations were used in calculating magnitudes.

For all other events, both types of coda length were measured on each of the three stations utilized. Two duration magnitudes (one for each coda length) were then calculated for each event based on the equation derived for each station. Finally, for each event, calculated magnitudes from each station were averaged to calculate the final earthquake magnitude. This was done separately for both types of coda length.

Results

Forty-seven local events were recorded during approximately thirty-four days of continuous seismic monitoring (Figure 8 and Appendix 1). Calculated magnitudes from this study range from M_{dur} 1.1 to 3.4 M_{dur} (Appendix 1). Locations from *HypoInverse* yielded sixteen events within the bounds of the array, while the remainder were located within 150 km of these bounds. Focal depths were generally shallow (< 10 km). However, five events were found to have focal depths greater than 25 km, and three events had calculated focal depths of greater than 40 km. In the study area, a depth of 40 km is approximately the depth to the Moho, and it is highly unlikely that any microseismic events occurred below this depth. The other two events had calculated depths of 26.8 km and 34.5 km, which *HypoInverse* could be interpreting correctly. Additionally, the root mean square residual (RMS) errors generated by *HypoInverse* were quite large for three other events (15.07, 15.49, and 25.84 seconds). This could be related to large timing errors or to wave travel paths in which the velocity model is inadequate (Klein, 1978). Events that displayed either great depth or high RMS error were not analyzed any further.

Four concentrated linear patterns of events were recognized and explored in greater detail. The first, a forty-two kilometer linear pattern of nine events trending approximately N60˚E appears about sixty kilometers west of the western array boundary. The second linear pattern of three events lies perpendicular to and intersecting this first linear pattern (trending approximately N30˚W). One event overlaps these two patterns. Notably, mapped faults from Tweto (1979) possess nearly the same trends and are in close proximity geographically to these perpendicular linear patterns of events (Figure 9).

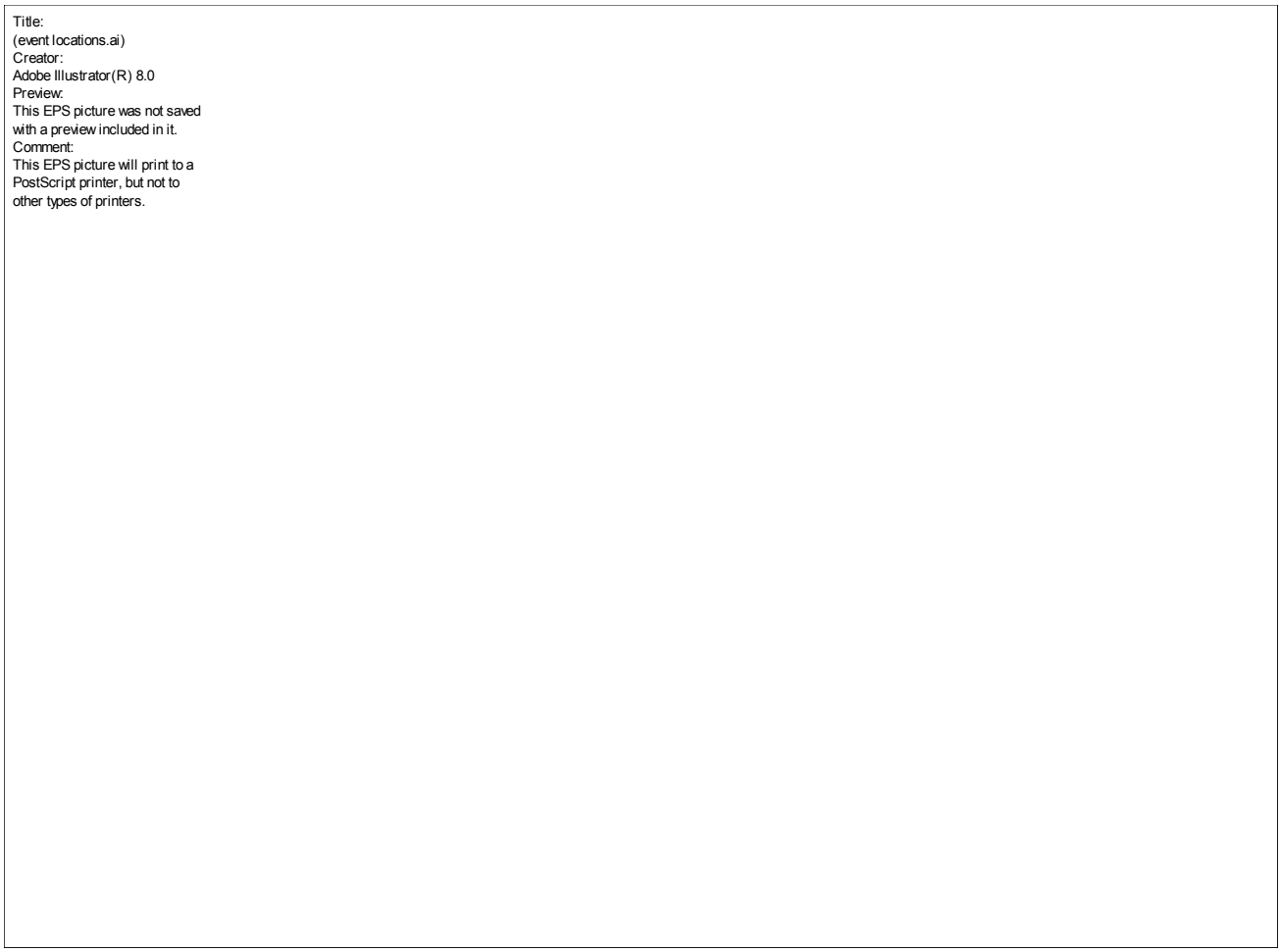

Figure 8. Map of event locations and mapped faults from Tweto (1979).

The linear pattern trending northeast-southwest appears to have a bimodal distribution of focal depths. Represented along this trend are very shallow events (≤ 0.3 km deep) and somewhat deeper events (between 2.4 and 9.4 km deep). However, the three events perpendicular to the first trend (trending northwest-southeast) range from 2.4 to 8.1 km in depth.

The final two concentrated linear patterns of events appear slightly west of the center of the array (Figure 10). Geologically, they are situated in the valley between the northern Front Range and the Park Range. Both patterns contain three events with one event in common. The first pattern of interest trends approximately N10˚W while the second trends approximately N70˚W. Mapped faults from Tweto (1979) in the area trend from north-northwest to west-northwest, and generally follow the trend of the linear patterns. Focal depths of these events range from 1.1 to 10.4 km.

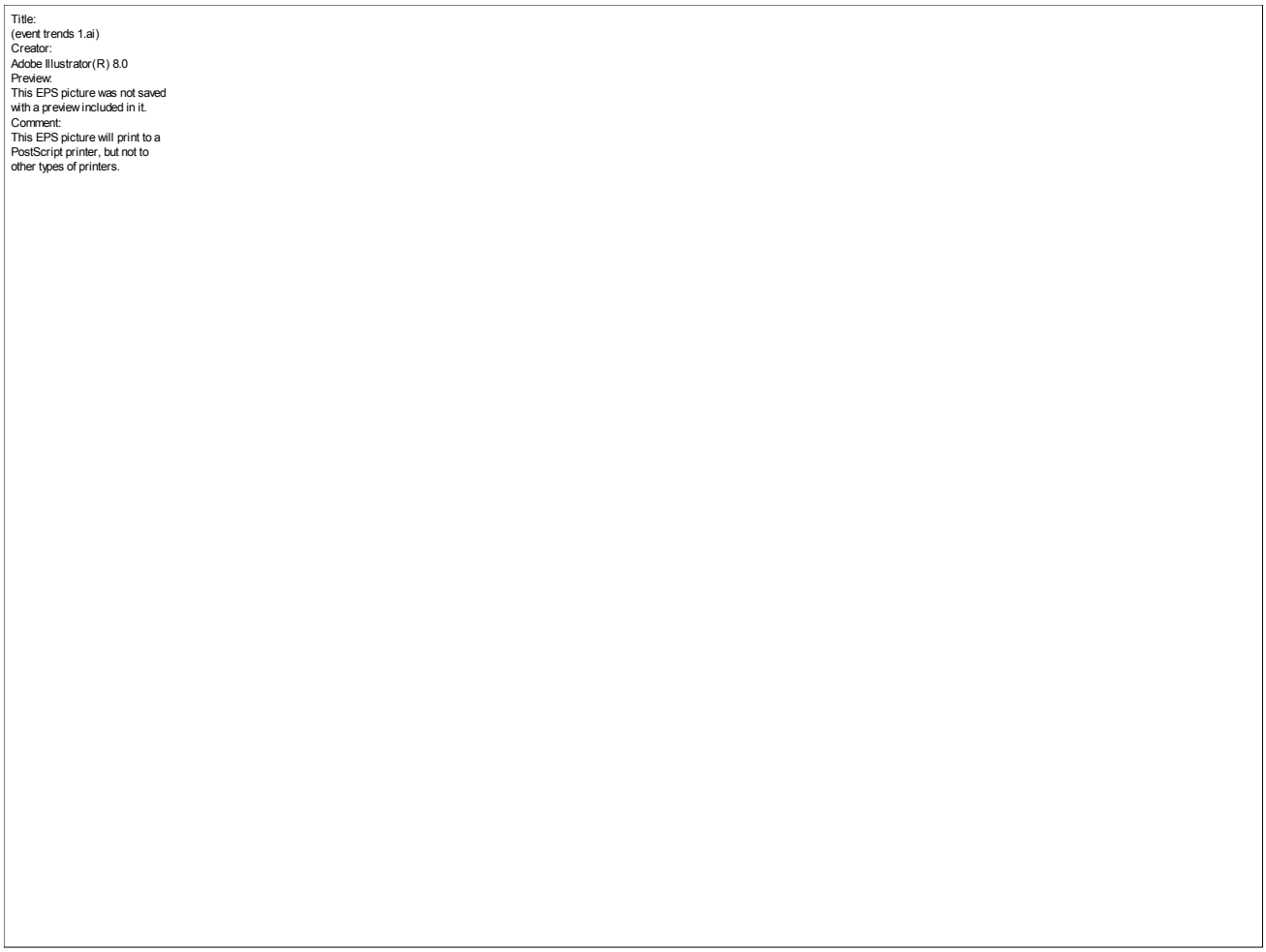

Figure 9. Map of two perpendicular event trends and mapped faults from Tweto (1979). Proposed stress field from Zoback and Zoback (1989) and the general orientation of faults in the Colorado lineament (Warner, 1978) are also shown.

Two events are coincident with one another and locate directly on Interstate Highway 80. Focal depths of these events are very shallow (0.03 and 0.11 km) and they have calculated magnitude values of 2.2 (M_{dur}) and 2.8 (M_{dur}). This may indicate an unnatural source (e.g., highway construction basting) for these events.

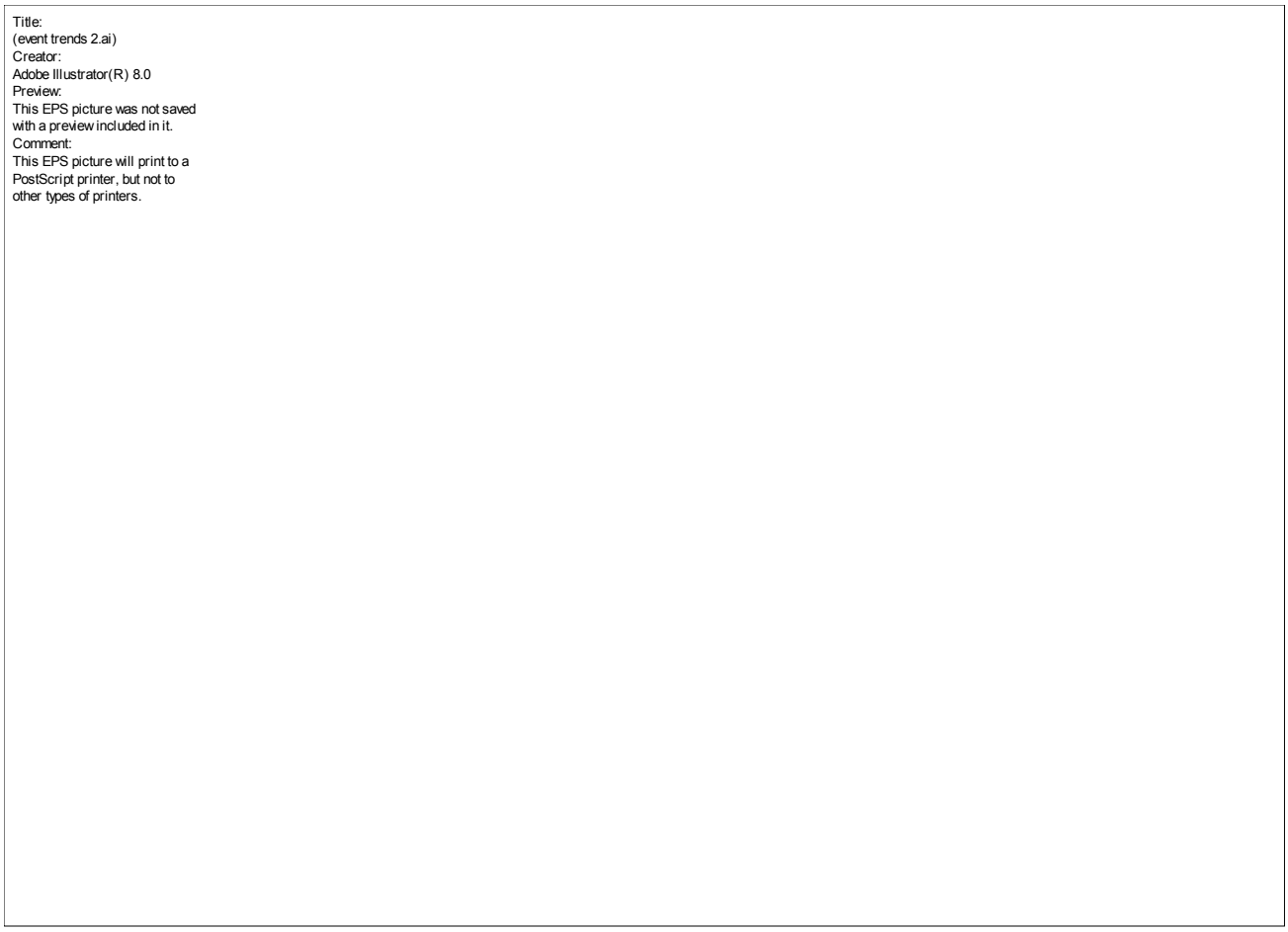

Figure 10. Map of a second set of event trends with faults from Tweto (1979) and the proposed stress field from Zoback and Zoback (1989).

Discussion

The general trends of the multiple linear patterns of events and their proximity to the faults mapped by Tweto (1979) suggest that these events were produced by slip along certain faults. Particularly, the events positioned to the west of the array show well defined trends with mapped faults lying very close to, or on top of, events in some cases. However, the linear trends near the center of the array do not follow particular mapped faults, but are probably related to nearby faulting.

As noted previously, two trends of the linear events west of the array are perpendicular and intersecting. Figure 9 shows both the stress field from Zoback and Zoback (1989) proposed for the Denver area and the general trend of the Colorado lineament. The linear pattern of events trending approximately N60˚E suggests two important observations. First, this pattern of events

lies seventy degrees from the direction of maximum horizontal compressive stress, or twenty degrees from the extension direction. Clearly, the trend of this pattern with respect to the proposed stress field is consistent with slip along a fault oriented parallel to the trend of the linear pattern of events. Consequently, if these earthquake patterns are delineating fault movement, then stress field orientation in north-central can be further constrained. Second, the trend of the pattern of events is nearly parallel to the general trend of the Colorado lineament. This observation implies that reactivation along this pre-existing trend of faults is likely to have produced this linear pattern. Given that both of these linear patterns were created in the modern stress field, it is likely that the orientation of the modern stress field is nearly coincident with the stress field proposed by Zoback and Zoback (1989) for the Denver area. In addition, four events within this trend have depths between 2.4 and 9.4 km, which most probably denote slip along a pre-existing fracture in Precambrian rock.

The second of the two linear patterns of events located west of the array trends approximately N30˚W. Again, this pattern lies twenty degrees from the maximum horizontal compressive stress axis, which is also consistent with slip along a fault oriented parallel to the trend of the linear pattern of events. These events all originate at depths between 2.4 and 8.1 km and also suggest reactivation along pre-existing fractures.

The same analysis can be applied to the two linear patterns of events located near the center of the array, although with less certainty. These patterns do not possess the same kind of linear density in which the events west of the array do. However, the linear pattern of events trending N10˚W are parallel to the maximum horizontal compressive stress axis or perpendicular to the extension direction. Consequently, this observation shows that normal slip probably is accommodating stress along the trend delineated by this linear trend of events. The other linear pattern of events trending approximately N70˚W is also consistent with reactivation of a pre-existing fracture. All five events are of significant depth (1.1 to 10.4 km) and could possibly be related to reactivation of Precambrian basement fractures.

Recently, an open-file report citing all faults with recognized Quaternary fault movement in Colorado was published by the Colorado Geological Survey (Widmann et al., 1998). There was no mention of active fault motion near any of these linear patterns of events. Consequently, it is not yet recognized that either of these two areas possess any active fault movements, but the evidence presented previously suggests that this is the case.

References Cited

Bott, J.D.J., and Wong, I.G., 1995, The 1986 Crested Butte earthquake swarm and its implications for seismogenesis in Colorado: Bulletin of the Seismological Society of America, v. 85, no. 5, p. 1495-1500.

Bott, J.D.J., Wong, I.G., Ake, J., Unruh, J., Nicholl, J., and Butler, D., 1996, Contemporary seismicity of the central Front Range, Colorado: Geological Society of America Abstracts with Programs, v. 28, no. 7, A283.

Brill, K.G., and Nuttli, O.W., 1983, Seismicity of the Colorado lineament: Geology, v. 11, p. 20-24.

Evans, D.M., 1966, The Denver earthquakes and the Rocky Mountain Arsenal disposal well: Mountain Geologist, v. 3, p. 23-26.

Fowler, C.M.R., 1990, The solid earth: An introduction to global geophysics: New York, Cambridge University Press, 427 p.

Goter, S.K., Presgrave, B.W., Henrissey, R.F., and Langer, C.L., 1988, The Carbondale, Colorado earthquake swarm of April-May 1984: United States Geological Survey Open-File Report 88-417, 8 p.

Healy, J.R., Rubey, W.W., Griggs, D.T., and Raleigh, C.B., 1968, The Denver earthquakes: Science, v. 161, p. 1301-1310.

Herrmann, R.B., Park, S.-K., and Wang, C.-Y., 1981, The Denver earthquakes of 1967-1968: Bulletin of the Seismological Society of America, v. 71, no. 3, p. 731-745.

Hughes, N.D., 1997, Results of a microseismic survey of the Front Range of Colorado: National Conference on Undergraduate Research—Proceedings, v. 11, p. 1857-1861.

Kirkham, R.M., and Rogers, W.P., 1986, An interpretation of the November 7, 1882 Colorado earthquake, *in* Rogers, W.P., and Kirkham, R.M., eds., Contributions to Colorado seismicity and tectonics—a 1986 update: Colorado Geological Survey Special Publication, v. 28, p. 122-144.

Klein, F.W., 1978, Hypocenter location program—*HypoInverse*—part 1: Users guide to versions 1, 2, 3, and 4: United States Geological Survey Open-File Report 78-694, 42 p.

Lee, W.H.K., and Stewart, S.W., 1981, Principles and Applications of Microearthquake Networks: New York, Academic Press, 293 p.

McGuire, R.C., Krusi, A., and Oaks, S.D., 1982, The Colorado earthquake of November 7, 1882: size, epicentral location, intensities, and possible causative fault: Mountain Geologist, v. 19, p. 1-23.

Sheehan, A.F., 2000, Microearthquake study of the Colorado Front Range: Combining research and teaching in seismology: Seismological Research Letters, v. 71, no. 2, p. 26-30.

Spence, W., Langer, C.J., and Choy, G.L., 1996, Rare, large earthquakes at the Laramide deformation front—Colorado (1882) and Wyoming (1984): Bulletin of the Seismological Society of America, v. 86, no. 6, p. 1804-1819.

Tweto, O., 1979, Geologic map of Colorado: United States Geologic Survey Special Map G77115, Scale 1:500,000.

Warner, L.A., 1978, The Colorado lineament: a middle Precambrian wrench fault system: Geological Society of America Bulletin, v. 89, p. 161-171.

Widmann, B.L., Kirkham, R.M., and Rogers, W.P., 1998, Preliminary Quaternary fault and fold map and database of Colorado: Colorado Geologic Survey Open-File Report 98-9, 331 p.

Wong, I.G., 1991, The 1986 Crested Butte, Colorado earthquake swarm: Mountain Geologist, v. 28, p. 3-8.

Wong, I.G., Bott, J.D.J., and Ake, J., 1994, Earthquakes and tectonic stresses in western Colorado: Geological Society of America Abstracts with Programs, v. 26, no. 6, p. 69.

Wong, I.G., Bott J.D.J., Ake J., and Unruh J., 1996, Earthquake hazard in central Colorado: Geological Society of America Abstracts with Programs, v. 28, no. 7, A283.

Zoback, M.L., and Zoback M.D., 1989, Tectonic stress field in the continental United States, *in* Pakiser, L.C., and Mooney, W.D., eds., Geophysical Framework of the Continental United States: Geological Society of America Memoir, v. 172, p. 523-540.

Appendix 1

Hypoinverse locations of picked events with calculated magnitudes. Magnitude 1 is either a calculated USGS magnitude (M_L) or a calculated duration magnitude (M_{dur}) in which the coda length runs from the P-wave arrival to the point at which the event can no longer be distinguished from the background noise. Magnitude 2 is calculated duration magnitude in which the coda length begins with the p-wave arrival and ends when the signal falls to twice the level of the background noise.

Date (Day-Month)	Origin Time (hh.mm.ss.ss; UTC)	Latitude	Longitude	Depth (km)	Magnitude 1	Magnitude 2
22-Jun	16.07.28.13	40.5667	-107.7283	8.12	2.2 M_{dur}	2.3 M_{dur}
23-Jun	19.08.59.96	41.3655	-106.4367	0.88	3.1 M_{dur}	3.0 M_{dur}
23-Jun	22.28.29.78	40.7742	-107.9612	7.05	2.0 M_{dur}	2.0 M_{dur}
24-Jun	20.46.39.97	40.3547	-107.3083	4.82	2.5 M_{dur}	2.5 M_{dur}
24-Jun	21.13.27.07	40.5413	-106.3460	1.10	2.6 M_{dur}	2.7 M_{dur}
25-Jun	06.35.14.41	42.0645	-106.2488	0.01	2.6 M_{dur}	2.1 M_{dur}
25-Jun	22.05.19.05	40.2775	-107.8503	0.05	3.0 M_{dur}	2.8 M_{dur}
26-Jun	23.56.44.61	40.2067	-106.5693	7.01	2.8 M_{dur}	2.8 M_{dur}
27-Jun	19.52.33.90	41.6233	-108.5263	0.11	2.8 M_{dur}	2.9 M_{dur}
28-Jun	10.25.11.37	41.6333	-106.7837	7.37	2.0 M_{dur}	1.7 M_{dur}
28-Jun	18.17.05.42	41.5840	-108.6962	0.03	3.0 M_{dur}	2.6 M_{dur}
29-Jun	12.52.24.28	41.3105	-107.1493	7.00	2.6 M_{dur}	2.8 M_{dur}
29-Jun	19.34.43.10	42.0600	-105.7395	0.11	2.7 M_{dur}	2.7 M_{dur}
1-Jul	22.05.10.85	40.7467	-106.3758	3.22	2.8 M_{dur}	2.7 M_{dur}
1-Jul	22.20.43.12	40.6228	-106.6100	10.37	2.6 M_{dur}	2.7 M_{dur}
2-Jul	11.49.14.46	42.0200	-106.1922	16.57		
2-Jul	15.46.54.28	41.6385	-108.5320	0.03	2.2 M_{dur}	2.0 M_{dur}
2-Jul	18.15.53.00	40.9528	-107.3863	9.05	2.0 M_{dur}	2.1 M_{dur}
3-Jul	05.13.06.07	42.1053	-106.5613	26.75		
3-Jul	05.41.59.59	41.3048	-106.2832	34.53		
4-Jul	21.57.27.75	40.2152	-107.8888	0.03	3.0 M_{dur}	2.9 M_{dur}
4-Jul	14.37.52.25	41.3455	-107.1558	0.11	2.9 M_{dur}	3.1 M_{dur}
5-Jul	22.09.37.87	40.3213	-107.6307	9.37	3.2 M_{dur}	3.0 M_{dur}
6-Jul	22.01.52.28	40.1973	-107.8968	0.20	1.7 M_{dur}	1.8 M_{dur}
6-Jul	22.06.24.26	40.1473	-107.0973	15.24	3.2 M_{dur}	3.2 M_{dur}
7-Jul	15.15.32.67	40.5655	-106.4513	8.56		
7-Jul	20.19.29.45	40.8365	-107.2052	0.11	2.7 M_{dur}	2.5 M_{dur}
7-Jul	22.03.00.99	40.3167	-107.6907	7.00	1.6 M_{dur}	1.4 M_{dur}
8-Jul	19.12.53.42	45.4233	-105.6243	7.00	3.4 M_{dur}	3.4 M_{dur}
8-Jul	20.24.13.30	40.4790	-107.6765	7.35	2.7 M_{dur}	2.7 M_{dur}
8-Jul	21.58.07.03	40.2637	-107.7685	6.90	2.7 M_{dur}	2.7 M_{dur}
11-Jul	23.11.35.30	41.0507	-105.1957	7.00	2.8 M_{dur}	2.7 M_{dur}
Date (Day-Month)	Origin Time (hh.mm.ss.ss;	Latitude	Longitude	Depth (km)	Magnitude 1	Magnitude 2

	UTC)					
12-Jul	22.00.24.24	40.2740	-107.7983	0.03	2.6 M_{dur}	2.8 M_{dur}
15-Jul	19.26.30.13	40.4442	-107.5277	0.27	2.9 M_{dur}	2.9 M_{dur}
16-Jul	21.35.10.82	40.6667	-106.3792	5.48	1.3 M_{dur}	1.1 M_{dur}
18-Jul	15.12.55.27	41.2658	-105.9643	15.62	3.3 M_{dur}	3.3 M_{dur}
18-Jul	22.25.28.45	40.3557	-107.5647	2.41	2.6 M_{dur}	2.6 M_{dur}
19-Jul	04.17.51.63	42.1347	-108.8183	7.00	1.6 M_{dur}	1.5 M_{dur}
19-Jul	10.27.09.75	40.8680	-108.5152	0.05	2.9 M_{dur}	2.9 M_{dur}
20-Jul	20.15.02.76	41.1682	-106.6095	0.11		
21-Jul	02.36.27.49	41.4525	-107.1168	13.21	2.8 M_L	